# *In situ* microbial metabolism as a cause of gas anomalies in ice

**Robert A. Rohde, P. Buford Price*, Ryan C. Bay, and Nathan E. Bramall†**

Physics Department, University of California, Berkeley, CA 94720

Contributed by P. Buford Price, April 21, 2008 (sent for review January 23, 2008)

**Isolated spikes of anomalously high concentrations of $N_2O$ have been reported at depths in Greenland and Antarctic ice cores corresponding to narrow time intervals over the past ≈$10^5$ years. Now, using a calibrated spectrofluorimeter to map protein-bound Trp, a proxy for microbes, versus depth in the 3,053-m GISP2 ice core, we find six depths at which localized spikes of high cell concentrations coincide with $N_2O$ spikes. We show that the excess gases are consistent with accumulation of *in situ* metabolic wastes during residence times of the excess microbes in the ice. Because of sparseness of $N_2O$ measurements and our spectrofluorimetry versus depth, the total number of microbially produced $N_2O$ spikes in GISP2 is probably much larger than six. Spikes of excess methanogens coincident with $CH_4$ spikes are found at three depths in the bottom 3% of GISP2, most likely because of methanogenic metabolism in the underlying silty ice, followed by turbulent flow of the lowest ≈90 m of ice. The apparent rates of *in situ* production of $N_2O$ and $CH_4$ spikes by metabolism are observed to be consistent with a single activation energy, *U*, and maintain proportionality to exp(−*U*/*RT*) over the entire temperature range down to −40°C. Fluorescence of nonmicrobial aerosols in GISP2 ice is distinguishable from microbial fluorescence by its different emission spectra. Our spectrofluorimetric scans throughout the GISP2 ice core lead us to conclude that both microbes and nonmicrobial aerosols are deposited in discontinuous bursts, which may provide a tool for studying wind storms in the distant past.**

climate | ice cores | proxy for dust storms | scanning fluorimetry | $N_2O$

The record of atmospheric gases such as $CO_2$, $CH_4$, $N_2O$, and $\delta^{18}O$ frozen in glacial ice provides a generally quite accurate record of Earth's climate over the last $10^5$ to $10^6$ years. Recently, it has been found that glacial ice also holds a record of past microbial diversity (1, 2). Because of their labor-intensive nature, direct counts of microbial concentrations, live/dead tests, and identification of taxa by molecular methods have been carried out at only a relatively small number of depths, leaving questions such as possible correlations of microbial deposition rates in ice with climate unanswered. In a few cases (3, 4), evidence has been found that unusually high concentrations of microbes living at isolated depths in glacial ice produce gaseous metabolic products that have distorted the climate record of those gases. In this article, we show that scanning spectrofluorimetry can rapidly measure the depth-dependent concentration of protein-bound Trp at submillimeter intervals throughout several thousand meters of ice cores in a cold repository such as the National Ice Core Laboratory (NICL). Analysis of shapes of autofluorescence emission spectra allows Trp, usually diagnostic of microbes, to be distinguished from other organic and mineral aerosols. In those cases, intensities are converted to microbial concentrations by making direct counts and measurements of cell sizes at several depths in ice samples where high intensities are found. Herein, we demonstrate the power of the scanning fluorescence technique by showing that microbes are deposited onto glacial ice in discontinuous bursts and that upward spikes in $N_2O$ at a number of depths in GISP2 ice correspond precisely with upward spikes of Trp fluorescence.

We used a six-channel TUCS fluorimeter with 224-nm excitation to obtain high-resolution maps of microbial cells in selected lengths of the GISP2 ice core via Trp autofluorescence. We divided the TUCS spectra into those spectra with shapes highly correlated with Trp autofluorescence (e.g., maximum emission intensity at 320–340 nm), which is the dominant response for microbial fluorescence, versus those spectra with maximum intensity at other wavelengths [consistent with dissolved organic matter (DOM) from oceanic sources or with mineral dust from terrestrial sources]. Free proteins in aerosols containing organic matter not associated with cells also contribute to Trp-like fluorescence, which cannot be distinguished from fluorescence attributed to proteins in cells. The continuous low-intensity background of Trp-like fluorescence in Fig. 1 may be due, in part, to free proteins.

In Fig. 1 and supporting information (SI) Fig. S1, red points denote microbial fluorescence (correlation factor $R \geq 0.75$)and blue points denote nonmicrobial fluorescence ($R < 0.75$). In a scan along a 13.5-cm-diameter core, the fraction of the core volume illuminated by the laser fluorimeter is only $\approx 4 \times 10^{-5}$. Thus, even if the laser beam were to damage some microbes, a strip along which scanning took place could be marked for avoidance by those who want to study cells in that particular core.

**Narrow Spikes of High-Microbial Concentration Correspond to Spikes of High $N_2O$ and $CH_4$ Concentration.** Fig. 1 shows examples of bursts of high intensity due to protein-bound Trp (red points) and nonmicrobial fluorescence (blue points). The sources of the aerosols in the WAIS ice core (Fig. 1*a*) probably come from the Southern Ocean and southern desert sources, whereas those in the GISP2 ice (Fig. 1*b*) probably come from the Arctic Ocean and East Asian deserts. High-amplitude, short depth-scale variability is a common feature of fluorescence measurements at all depths on ice cores. Our fluorescence data somewhat resemble the data in Fig. 1*c* of Prospero *et al.* (5), which show a spiky time variability of both dust and windborne culturable bacteria crossing the Atlantic Ocean from Africa to Barbados. In all three cases, the transport of microbes to the ice sheet is likely to be shaped by weather patterns varying on seasonal and interannual scales. This variability complicates our analyses in that microbial deposition on ice occurs in bursts sometimes extending only a few centimeters in depth.

Flückiger *et al.* (6, 7) and Spahni *et al.* (8) called attention to the occurrence of anomalously high $N_2O$ concentrations, termed "gas artifacts," at isolated points in their $N_2O$ data in Greenland ice cores (GRIP and NGRIP) and East Antarctic ice cores (Dome C). Flückiger (9) suggested that among the possible explanations for isolated high-$N_2O$ points might be *in situ* metabolism by nitrifying or denitrifying bacteria. Independently, Sowers (3) found excess $N_2O$ at ≈2,000-m depth in the Vostok ice core, and Campen *et al.*

Author contributions: P.B.P. designed research; R.A.R. and P.B.P. performed research; R.A.R., R.C.B., and N.E.B. contributed new reagents/analytic tools; R.A.R. and P.B.P. analyzed data; and R.A.R. and P.B.P. wrote the paper.

The authors declare no conflict of interest.

*To whom correspondence should be addressed. E-mail: bprice@berkeley.edu.

†Present address: National Aeronautics and Space Administration Ames Research Center, Moffett Field, CA 14035.

This article contains supporting information online at www.pnas.org/cgi/content/full/0803763105/DCSupplemental.

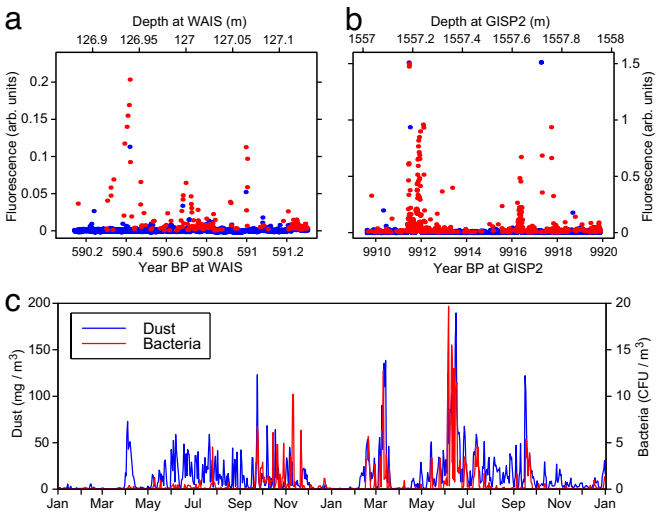


**Fig. 1.** Intensities of Trp fluorescence (red points) and non-Trp fluorescence (blue points) versus age. (*a*) WAIS ice at ≈127 m depth. (*b*) GISP2 ice at 1,557 m. Spectra were taken at ≈300-$\mu$m intervals along each core scanned; full spectra for all points are stored in memory. (*c*) For comparison, the rate of arrival of bacteria (red points) and dust (blue points) blown from African desert sources to an air collector on Barbados (5) during a 2-year period (1996 and 1997).

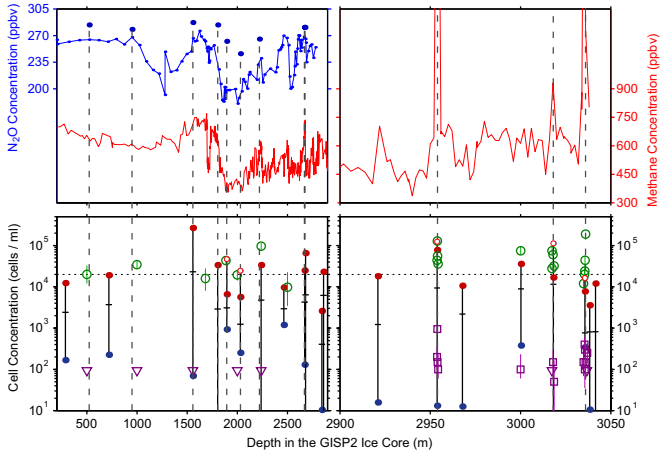


**Fig. 2.** Depth dependence of $N_2O$ (13) and $CH_4$ (14, 15) concentrations (*Upper*) and of microbial concentrations (*Lower*) inferred from our scans of protein-bound Trp fluorescence (proxy for microbial cells) and from direct counts of methanogens by F420 epifluorescence microscopy in the GISP2 ice core. Red points above the horizontal dashed line show excess Trp; green circles above the dashed line are excess cells by direct counts.

(10) found excess $CH_4$, $N_2O$, $CO_2$, and $\delta^{18}O$ of $O_2$ at a depth ≈17 m above bedrock in the Sajama (Bolivia) ice core. Both groups suggested that microbes metabolizing *in situ* might account for the anomalously high values. Direct evidence for *in situ* microbial metabolism was presented by Tung *et al*. (11), who tied excess $CH_4$ in three narrow regions in the bottom 90 m of GISP2 with large narrow excesses in their direct cell counts stained with Syto-23 and methanogens observed by their F420 autofluorescence. These excesses of cells, methanogens, and methane coincided in depth to within 0.1 m, the small uncertainty being due to the difficulty of matching depths of samples sent to more than one laboratory for analysis. They occurred in clear ice rather than in the silty basal ice known to have excess gases and high microbial counts (12).

We make the case that some or even most of the narrow spikes of excess gas are products of *in-ice* microbial metabolism, and we use "gas spike" instead of "gas artifact," which would imply a measurement error of unknown origin. During a 2-week period that we were allotted at NICL, we scanned cores in GISP2 ice both at depths near where one or more gas spikes had been found and at random depths. When we found that a microbial excess based on Trp fluorescence extended over an entire 1-m core section, we scanned sections just above and below the one with the excess to measure its full extent.

Fig. 2 reduces the data to a compact form that facilitates comparison of our fluorescence data with gas concentrations. Fig. 2 *Upper* shows concentrations of $N_2O$ by Sowers (13) and of $CH_4$ by Brook *et al*. (14, 15) as a function of depth in GISP2 ice cores; Fig. 2 *Lower* shows a capsule summary of our $>10^5$ data on concentrations of microbial cells and methanogens. For the $N_2O$ data (*Upper Left*), we have pulled out a number of Sowers' measurements (shown as points above the blue curve) that appeared to be artifacts when compared to neighboring points and to our expectations based on the absence of corresponding variations in $CH_4$ (red curve). We marked the locations of those putative gas spikes with vertical dashed lines. The three vertical lines at 2,954, 3,018, and 3,036 m (within 90 m of bedrock) mark regions of anomalously high $CH_4$ concentrations.

We investigated cell concentrations inferred from Trp fluorimetry in 20 regions ranging from a few decimeters to a few meters in depth. The data along any meter-long portion of core are usually highly variable on decimeter scales. To demonstrate that variability, we constructed running 5-cm averages for Trp-based cell concentration in each of the 20 1-m-long regions and connected the highest and lowest 5-cm block with a vertical line bounded by red and blue points in Fig. 2 *Lower*. The crossing mark on each vertical line indicates the average cell concentration in that region of the core. We chose 5-cm intervals because gas data are usually measured in ice samples 5–10 cm thick. We generally excluded measurements from within 5 cm of the cuts between core segments because the ends often show higher Trp-based fluorescence, possibly indicating contamination after the core was cut or broken. Exceptions (shown as small, open red circles) were made in cases where we knew that anomalous gas measurements had been collected from regions within 5 cm of a core cut or break. In those cases, we included the high cell concentrations found near the edges.

Fig. 2 includes as open symbols direct counts by our group (11) of cell concentrations and methanogen concentrations. Large open circles denote total cell concentrations, open squares denote methanogen concentrations, and open triangles denote upper limits at 84% confidence level on methanogen concentrations, where we found no cells in 0.02 $cm^2$. We note that the use of epifluorescence microscopy to image the green autofluorescence of F420 is accepted as a unique signature of methanogens (16–18), and intensity of F420 fluorescence scales with biomass for a given taxon (19).

The $N_2O$ spikes are distributed throughout the depths for which measurements were made. By contrast, the three $CH_4$ spikes occur only at 2,954, 3,018, and 3,036 m, within 90 m of the silty ice at 3,041–3,053 m. F420 counts of methanogens with epifluorescence microscopy at three depths both above and below the $CH_4$ spikes showed that excess methanogens are localized at exactly those depths, each with SD ≈0.1 m in their depth distribution.

Comparing Fig. 2 *Upper* and *Lower*, we see that high levels of Trp and F420 fluorescence indicated by red points are generally associated with the spikes of excess $N_2O$ and $CH_4$. All depths with $>3 \times 10^4$ cells/$cm^3$ (either from Trp or cell counts) corresponded to gas spikes; all depths with >150 F420 counts corresponded to $CH_4$ spikes. The blue points are included simply to show that the fluorescence at depths just above and below the depths where Trp peaks occur is far weaker. Direct counts (green points) at depths where $CH_4$ spikes had been found (2,954, 3,018, and 3,036 m) showed very high values. Of the direct counts at random depths, those at 2,238 and 3,000 m also showed very high values that were confirmed by Trp fluorescence, whereas those at other depths did

not. Because of the shortage of time allotted to us at NICL, we did not examine all of the putative gas spikes, and we have a limited set of control measurements from regions with normal gas concentrations. The average depth intervals between measurements of $N_2O$ and $CH_4$ were so large (for $N_2O$, 24.6 m per point; for $CH_4$, 6.2 m per point at 200 to 2,900 m and 2.45 m per point at 2,900 to 3,040 m) that a number of gas spikes are likely to have been missed. For $N_2O$, we judged ≈10% of the measurements (9 of 91 measurements >400 m deep) to be anomalous, and so we measured Trp fluorescence in and around those depths. If the fluctuating cell concentrations we observed as spanning several orders of magnitude are common throughout the core, then it is plausible that the gas spikes occurred when high cell concentrations were sampled merely by accident. The excess methane, localized only in the deepest portion of the core, suggests a more complex story that is discussed below.

Because the concentration of atmospheric $CO_2$ trapped in ice is nearly three orders of magnitude higher than the concentrations of $CH_4$ and $N_2O$, spikes of $CO_2$ due to *in situ* microbial metabolism are unlikely to be detectable except in ice containing orders of magnitude higher microbial concentrations than in our current experiments. In only two cases have $CO_2$ excesses been attributed to *in situ* microbial metabolism. First, in the GISP2 silty basal ice, where $CO_2$ is a factor ≈500 higher than atmospheric and $CH_4$ is a factor $\approx 10^4$ higher than atmospheric (20), our group (12) found extremely high concentrations of cells ($10^8 - 10^{10}$ cm$^{-3}$), using direct counts of Syto23-stained cells and of methanogens ($10^6 - 10^8$ cm$^{-3}$) using direct counts of F420. Almost all of those cells were attached to the $10^{-3}$ to $10^{-2}$ g/g of silt grains. Second, in the basal ice at GRIP, ≈30 km from GISP2, Souchez *et al*. (21) found very large concentrations of $CO_2$ and $CH_4$, as well as greatly enhanced $\delta^{18}O$ of $O_2$. They suggested that *in situ* respiration may account for those excesses.

**Temperature-Dependent Metabolic Rate in Greenland Ice.** Price and Sowers (4) developed a powerful method for measuring the temperature-dependent average metabolic rate of living microbes trapped in ice or rock. They showed that if all of their metabolic waste gas is trapped within the region occupied by the excess microbes, the metabolic rate $\mu_i(T)$ in weight fraction of cellular carbon turned over per year is proportional to $Y_i g_i / f_i n_i m_i t$.

Here, $Y_i$ is the yield of gaseous metabolic product of type $i$, $g_i$ is the fraction of metabolic products leading to carbon, $n_i$ is the concentration of living, metabolizing microbes of type $i$, $f_i$ is the fraction of microbes producing gas of type $i$, $m_i$ is the average mass of carbon per cell of type $i$, $t$ is the storage time of the gas in the ice, and $T$ is the temperature in Kelvin at the depth for each excess microbial concentration. We ignored the temporal history of a microbial population's temperature and gas production rate, but we estimate that for the GISP2 ice not doing so introduces an error that is small compared to the other sources of uncertainty.

We present results for methanogens, which produce $CH_4$ only in the absence of $O_2$, and nitrifiers, which can generate $N_2O$ at low $O_2$ concentration by (*i*) reducing to $N_2O$ a fraction of the $NO_2^-$ that they generate by nitrifier denitrification, and (*ii*) by converting a small fraction of the intermediate $NH_2OH$ to $N_2O$ instead of $NO_2^-$ as a by-product. For microbial $N_2O$ production in Vostok ice, Sowers (3) reported peaks in $N_2O$ concentration and high values of $\delta^{15}N$ and low values of $\delta^{18}O$ at roughly the same depths where Abysov *et al*. (22) had found peaks in microbial concentration. Sowers concluded that the excess $N_2O$ was produced *in situ* dominantly by nitrifying bacteria, in contrast to production by denitrifying bacteria, which he found produces both excess $\delta^{15}N$ and excess $\delta^{18}O$. From measurements in Lake Bonney ice at depths where there was a strong excess of nitrifiers (23), together with calculations by Poughon *et al*. (24), we adopted the ratio $g_i$ = (C fixed)/($N_2O$ produced) = 0.04 to convert from the rate of nitrification to the rate of carbon turnover. In the absence of direct measurements, we assumed the same composition, $f_i = 0.04$, that was obtained for nitrifiers in Lake Bonney ice (23). We took $m_i = 24 \pm 5$ fg carbon per cell based on SEM measurements of average cell volume 0.144 $\mu$m$^3$ in GISP2 ice (12). For the calibrations, we made direct counts of Syto23-stained cells at five depths in GISP2 ice. We assume that the average fluorescence efficiency for the cells in the scans reported here is the same as for those cells.

For methanogens, $f_i = g_i = 1$ and $n_i$ was found by using F420 fluorescence. $F_{420}$ autofluorescence images of methanogens in the silty ice with epifluorescent microscopy were not sharp enough to make accurate size measurements. We adopted a carbon mass of 24 to 90 fg for methanogenic cells. The lower value was that of cells measured by SEM in GISP2 silty ice (12), and the upper value was from *Methanococcus jannaschii* cultures of 1 $\mu$m cocci.

Only microbes alive and able to metabolize produce the gases used in the calculation of metabolic rates in the ice. However, the protein fluorescence does not distinguish between living and dead microbes or between proteins not associated with cells. Following Miteva *et al*.,[‡] , who obtained values from ≈2.5% to ≈80% for the fraction alive when they used a live/dead stain for their direct counts of cells at various depths in the GISP2 clear ice and ≈85% for the fraction alive in the silty ice, we assume that the fraction of the metabolizing cells derived from the protein fluorescence scans is 50% at all depths. In Eq. **1**, the factor $n$ takes into account the fraction of cells alive and metabolizing at very low oxygen concentration.

Rohde and Price (25) showed that aerobes and strict anaerobes can coexist provided they are isolated in the ice lattice rather than in oxygen-rich veins. At depths below $\approx 10^3$ m in both Vostok and GISP2 ice, the air in bubbles has transformed into solid air-hydrate crystals (26), leaving an equilibium concentration of $\approx 2.4 \times 10^{-7}$ mole fraction $O_2$ dissolved in the lattice. We note that the diffusion rate of $H_2$ in ice is more than four orders of magnitude greater than that of $O_2$, which largely counteracts the differences in their atmospheric abundance. In a diffusion-limited microenvironment below the clathrate transition zone, microbes would receive approximately one molecule of $H_2$ for every two molecules of $O_2$. Because of the very low metabolic rates at subzero temperatures, the diffusion rates of nutrients and waste gases are sufficiently high that both aerobes and strict anaerobes can survive (25). Methanogens can survive in a microcommunity with aerobes, including nitrifiers, that deplete the $O_2$, and they express the enzymes catalase and superoxide dismutase to neutralize the toxic by-products of $O_2$ within their cells.

For $Y_i$ in ppbV relative to air, $m_i$ in fg, $t$ in years, and air content in the ice core at STP ≈0.09 cm$^3$ (g ice)$^{-1}$ for GISP2 ice (27), the metabolic rate becomes

$$\mu_i(\text{g C (g C)}^{-1}\ \text{yr}^{-1}) = 2.33\ g_i\ Y_i / f_i n\ m_i t \qquad [1]$$

For $N_2O$ and $CH_4$ production, $t$ is from refs. 13–15. For methanogenic production of $CH_4$ spikes, which we detected only in the stratigraphically disturbed ice at depths ≥2,954 m, age does not increase monotonically with depth. We used values from Suwa *et al*. (28), who reconstructed the ages at those depths by comparing measurements of $CH_4$ and $\delta^{18}O_{atm}$ in the disturbed section of the GRIP and GISP2 cores with the same properties in the Vostok ice core.

Fig. S2 shows that $Y/n$, the ratio of concentration of excess gas in a spike to the concentration of cells inferred from Trp fluorescence, increases by five orders of magnitude with depth. If the excess gases had been produced by microbial metabolism in the atmosphere or in sources such as wetlands, deserts, and oceans, there should have been no systematic change in $Y/n$ with depth during the $>10^5$ years of growth of the Greenland glacial ice. Instead, we assume that the

[‡]Miteva V, Sowers T, Brenchley JE, 11th International Symposium on Microbial Ecology, ISME-11, August 20–25, 2006, Vienna, Austria.

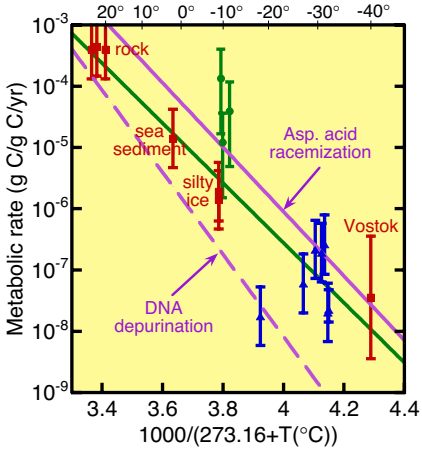


**Fig. 3.** Metabolic rates of fractional turnover of cellular carbon per year as a function of inverse temperature in Kelvin. Red squares are from ref. 4, green circles are for $CH_4$ production (ref. 11 and present data), and blue triangles are the present data for $N_2O$ production. The purple lines are extrapolated from rates of racemization of aspartic acid (29) and of DNA depurination (30), both measured at higher temperatures than shown. The green solid line is an exponential fit to the metabolic data.

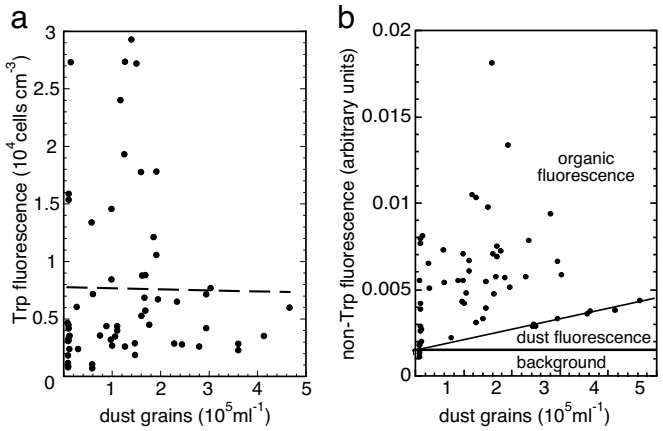


**Fig. 4.** Fluorescence as a function of dust concentration in GISP2 ice. (*a*) Cell concentration. (*b*) Non-Trp fluorescence.

excess gas was produced and fully retained in the ice by microbes undergoing *in situ* metabolism. With that assumption, the expression for metabolic rate is proportional to $Y/nt$.

The use of Eq. **1** leads to the results shown in Fig. 3, which also displays data analyzed in ref. 4 for rock and sea sediment, a data point for Vostok ice (4), and two points for GISP2 silty ice (12). The errors in Fig. 3 are mainly due to uncertainty in the fraction of cells metabolizing and, for methanogens, to the carbon mass. The large error for the Vostok ice calls attention to the fact that the $N_2O$ measurement (3) was displaced by several meters from the associated microbial measurement (22).

With the possible exception of the methane spikes, the gas spikes are accounted for by in-ice microbial metabolism at a rate proportional to $\exp(-U/RT)$, with activation energy $U$ in kJ/mol, a mean temperature $T$ in Kelvin, and $R$, the gas constant, in kJ/mol·K. The slope ($U \approx 94$ kJ/mol) and intercept of the best-fit line to our data are about the same as found earlier on the basis of the data points indicated by solid red squares (4). The solid purple line is an extrapolation of an Arrhenius line for laboratory measurements of the rate of spontaneous aspartic acid racemization in microbes in wet samples of Siberian permafrost at 100° to 144°C (29). The dashed purple line is an extrapolation of an Arrhenius line for DNA depurination measured in laboratory experiments (30).

As shown in Fig. 2, methanogens were detected by F420 imaging only in the disturbed ice. This finding leads to the conclusion that the methanogens were probably exhumed from the basal silt, rather than having fallen onto the ice from the atmosphere. However, the observation that each region of ice with a methanogen excess is clear and narrow in depth (<20 cm) limits the scenarios for mixing and uplift. The consistency of the methane excess with the methanogen excess also suggests that, regardless of the origin of the cells, the methane was probably produced *in situ*.

**Nonmicrobial Fluorescence in GISP2 Ice.** Fig. 4 compares the dependence of average cell concentration (inferred from Trp fluorescence) and of non-Trp fluorescence on mineral dust grain concentration (31, 32) in the same core length. For all times before the rise of agriculture, high dust concentration is a good proxy for low temperature (33, 34). In Fig. 4*a*, all of the points with >8,000 cells $cm^{-3}$ occur at times when the dust concentration was less than $\approx 2 \times 10^5$ grains $ml^{-1}$. Thus, our data suggest that large microbial concentrations correlate with warm temperatures, despite our prior expectation that deposition rate of microbes, along with other aerosols and with dust, would correlate with low temperature. More data are required before a strong conclusion can be reached.

For a rough categorization, the lines divide Fig. 4*b* into three labeled regions. Using the fact that most organic matter present in aerosols is much more strongly fluorescent than common mineral grains (35), we conjecture that the points with highest fluorescence intensity are due mainly to organic matter deposited from aerosols, with a minor contribution from weakly fluorescing mineral grains, labeled "dust fluorescence." Noting the existence of an event-free region at low fluorescence that expands with higher dust concentration, we suggest that the sloped line denotes the contribution from mineral grain fluorescence. Thirteen points fall closely on this line, which we attribute to the weak fluorescence of dust grains not containing organic aerosols. We attribute points above the line to contributions mainly from non-Trp organic aerosols transported onto the ice. From the slope of the line, we calculate that fluorescence intensity per dust grain is weaker than that per microbial cell by a factor of $\approx 10^2$. Taking into account the ratio of average cross-sectional area $\approx 3\ \mu m^2$ (32) of a dust grain to that of a $0.3\ \mu m^2$ cell as an estimate of relative absorption per particle, we conclude that the cell contributes $\approx 10^3$ times as much fluorescence per unit cross sectional area as a typical dust grain. This conclusion is consistent with Bramall's study (35) of 224-nm fluorescence of dust grains averaged over the minerals most commonly found in the study of GRIP dust grains (36).

With only six wavelength channels in the TUCS, we cannot uniquely identify the mineral grains that contribute to fluorescence. We find, however, that some of the weak non-Trp spectra are consistent with spectra of feldspar, calcite, pyrophyllite, volcanic rhyolite, and quartz, the most brightly fluorescent mineral species present in Greenland ice (35).

Complex noncellular organic matter, typically humic and fulvic acids, is usually the dominant organic constituent of marine aerosol particles, both in concentration (22 to 125 $\mu$M, according to ref. 37) and absorptivity, whereas tryptophan and tyrosine, as either free amino acids or proteins, in marine aerosol are negligible (<0.2–3 $\mu$M) by comparison (37). In a shallow WAIS (West Antarctica) ice core, John Priscu (private communication) measured organic matter at 12 depths from 71 to 128 m and found values from 24 to 295 $\mu$M of non-acid-purgeable organic carbon, consistent with the above values for marine aerosols. Using fluorescence excitation-emission matrices, Mopper and Schultz (38) found that the major component of DOM in the top $\approx$200 m of ocean water has an intensity maximum at $\lambda_{exc} \approx 225$ nm, with $\lambda_{em}$ decreasing monotonically out to $\approx$380 nm. We find that the most intense non-Trp fluorescence in single particles often shows a monotonic emission

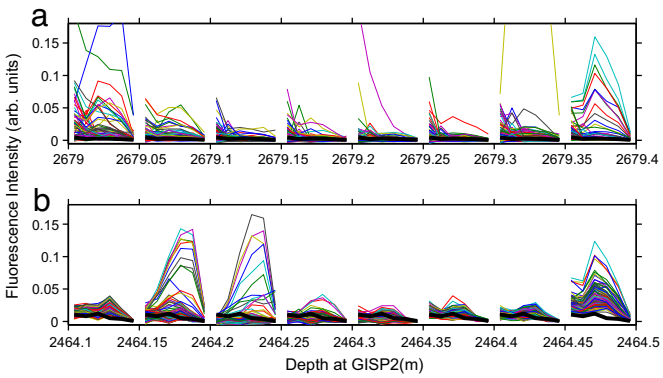


**Fig. 5.** Examples of non-Trp spectra in GISP2 ice. (*a*) Abrupt changes in spectral shapes in 5-cm (≈10-year) intervals at 2,679 m. (*b*) Abrupt changes in spectral shapes ≈2,464.24 m (5 cm ≈ 8 years) where the Z2 volcanic ash layer was found.

spectrum like that found by Mopper and Schultz. Examples in Fig. 5 are the monotonic green spectrum at 2,679.0 to 2,679.05 m and the purple spectrum at 2,679.2 to 2,679.25 m. Strong wind action is partly responsible for transporting organic matter from near-surface ocean waters in aerosols onto Greenland ice. Aerosol source locations should depend on glacial stage: The lowered sea level during glacial periods exposes new sources of mineral dust, whereas the reduced extent of sea ice during warm periods exposes new oceanic sources. Fig. 4*b* is consistent with these two effects: The sloped line increases with dust concentration, whereas the points above the sloped line suggest a correlation with low-dust (warm) periods. In GISP2 ice, the concentration of methanesulfonate, an aeolian decomposition product of dimethyl sulfide from dead phytoplankton, was much higher during warm than cold periods (39). This finding has been interpreted as having been due to the larger area of open ocean near Greenland during warm periods.

Fig. 5 gives examples of non-Trp spectra in GISP2 ice. Each spectrum displays fluorescence in six channels (from left to right: 300, 320, 340, 360, 380, and ≥420 nm). Fig. 5*a* shows ≈750 spectra in 5-cm depth intervals from 2,679.00 to 2,679.35 m. Fig. 5*b* shows ≈1,750 spectra at the Z2 volcanic ash band centered at 2,464.23 m. Both the amplitudes and shapes of the spectra at 2,464.15 to 2,464.25 m differ from those above and below the ash band. The nonmicrobial aerosol composition (organic matter plus mineral grains) changes dramatically in depth intervals as short as ≈5 cm, indicating abrupt changes on a time scale of years in aerosol sources.

## Discussion

At NICL, we collected $>10^5$ fluorescence spectra at 224-nm excitation, which allowed us to measure the fine-scale depth distribution, and thus arrival rate, of organic and inorganic aerosol particles transported onto the accumulating ice at Summit, Greenland. Our analysis of protein-bound Trp complements traditional biological assay techniques. Although it provides no information on taxa, it can inform microbiologists to within 300 $\mu$m where to analyze an ice sample that is greatly enriched in microbial cells. Simultaneously, the non-Trp spectra map the arrival rate of nonmicrobial material.

At an ice core storage facility with enough space to set up a translation stage, our fluorimeter can scan a 1-m core in 5 min, provided the core has a clean, flat surface, can be aligned horizontally ≈1 mm below the laser beam emission port, and is thick enough so that its other side is >1 cm below the region from which laser-induced fluorescence can reach the photon detectors.

We discovered that both microbes and nonmicrobial aerosols are deposited onto the ice in bursts that are discontinuous on a scale of millimeters to centimeters, corresponding to time intervals of seasonal to decadal. Bursts may serve as a proxy for storms during which the wind speed exceeds the local threshold for sweeping up dust and microbes from one or more regions. Kurosaki and Mikami (40) found that there is a sharp threshold wind speed for dust emission at East Asian desert and grassland sites. The concept of a threshold wind speed also applies to microbial and nonmicrobial emission from oceans. Our fluorimeters have the resolution to study the time distribution of bursts of high concentrations of microbes, organic matter, and dust extending $>10^5$ years back in time.

The depths of occurrence of gas spikes are thought by some to show a correlation with climate. For example, Spahni *et al.* (8) pointed out that the $N_2O$ spikes in Dome C occur at depth intervals that correlate strongly with high dust concentrations corresponding to glacial periods. To avoid interference of gas spikes with their climate study, they excluded $N_2O$ data at depths in Dome C with >300 parts per billion by weight of dust. The graphical summary of our data in Fig. 4 presents a somewhat different picture for Greenland ice. Spikes of high microbial concentration tend to occur at depths where the dust concentration is relatively low (Fig. 4*a*), as does nonmicrobial organic fluorescence (Fig. 4*b*), whereas mineral fluorescence increases with dust concentration. We are scheduled to scan all 3,465 m of the WAIS ice core as it arrives at NICL and to scan the NEEM ice as cores are removed and cut during drilling. This process will allow us to map the fluxes of microbial and nonmicrobial aerosols in both Arctic and Antarctic ice with high statistics over the last ≈150,000 years and to reach more definitive conclusions about the correlations between microbial and nonmicrobial concentrations and glacial period.

Gas spikes in undisturbed ice (shallower than ≈2,750 m) at GISP2 show up only in the $N_2O$ record. Because methanogens usually comprise no more than ≈1% of all microbes in ice, and the atmospheric concentration of $CH_4$ is nearly three times higher than that of $N_2O$, $CH_4$ spikes are far less likely to be detectable than $N_2O$ spikes. In Fig. 2, the F420 spikes occur only in disturbed regions, showing that methanogens and their $CH_4$ metabolic products may have been exhumed from the silty ice, probably under anaerobic conditions (12). The other known $CH_4$ spikes are those in the basal ice at GRIP (20), in the basal ice at Dye 3 (41), at a depth near bedrock in the alpine glacier Colle Gnifetti (42), and at a depth within ≈12 m of bedrock in the Sajama (Bolivia) glacier (10).

From the point of view of its value as a climate proxy, it is fortunate that the concentration of atmospheric $CO_2$ in the ice is so high relative to the microbial concentration that $CO_2$ excesses or deficiencies caused by *in situ* microbial metabolism are unlikely to be detectable except in basal ice that was formed on a highly concentrated microbial habitat, such as was present in wetland before glaciation.

Our data in Fig. 3 strengthen the evidence that microorganisms can live in ice at temperatures tens of degrees <0°C. The dashed Arrhenius line extrapolated to ice temperatures from laboratory data on racemization of amino acids at temperatures 100° to 144°C is within a factor two of our Arrhenius line for survival metabolism of microorganisms imprisoned in ice or rock. The dot-dashed Arrhenius line, extrapolated to low temperature from laboratory data on DNA depurination (29), is lower than our data, suggesting that less metabolic energy is required to repair DNA damage than racemization damage. The similarity of the racemization rate to the Arrhenius line for survival metabolism led Price and Sowers (4) to conjecture that microbes expend essentially all of their metabolic energy to repair spontaneous macromolecular damage, enabling them to stay alive as long as the nutrients last. For a habitat in which microbes depend on diffusion of nutrients through the ice lattice, the supply of small gaseous molecules such as $H_2$, $O_2$, $CO_2$, and $NH_3$ can maintain microbial life for as long as $10^6$ years at low temperature (25). In particular, methanogens can metabolize during the intervals between arrival of $O_2$ molecules by diffusion at subzero temperatures.

Our view of metabolism solely to repair spontaneous damage is consistent with the conclusion of Johnson *et al*. (43), based on their measurements of DNA degradation in ancient bacteria, that continuous metabolic activity with DNA repair via a host of repair pathways (44) is a more successful strategy for longevity than spore formation. The problem with spores is that repair does not begin until after they return to the vegetative state, in which case the accumulated damage may be too extensive for repair to be successful. We note that enzymatic activity has been detected in actinomycete spores at 40°C (45), which may indicate some capability for damage repair. However, Shafaat and Ponce (46) have shown that spores are only ≈1% as abundant as vegetative cells in GISP2 ice; at subzero temperature, the total rate of damage repair of spores is thus negligible relative to the rates shown by the purple lines in Fig. 3.

## Materials and Methods

We used a Photon Systems TUCS fluorimeter with six phototubes around a 224-nm laser and covered with bandpass filters at 300 ± 10, 320 ± 10, 340 ± 10, 360 ± 10, 380 ± 10, and ≥420 nm. The laser excites fluorescence of protein-bound Trp in a region of ice ≈0.5 cm deep with diameter ≈200 $\mu$m at 300-$\mu$m distance intervals. Fig. S1 shows fluorescence data that reveal how the TUCS distinguishes microbes from mineral grains. We chose ice cores that had been cut lengthwise on a band saw to a thickness of ≈7 cm and polished on the flat side. We scraped the flat side of each core with a microtome blade to remove ≈1 mm of ice. To take data, a fluorimeter was mounted with the exit point of the laser beam ≈1 mm above the ice surface.

Our methods of preparation of ice samples for extraction and treatment of microbial cells and our method of enumeration of methanogens and cells were identical to those described in ref. 11. We used epifluorescence microscopy to view the F420 autofluorescence of methanogens and the fluorescence of cells stained with Syto-23. In nonmethanogens, the concentration of F420 was too low to be detected without purification (18). With direct counts, we found that the microbial concentrations inferred from both the TUCS and F420 epifluorescence microscopy were peaked at 2,954, 3,018, and 3,036 m to within ≈0.1 m.

To relate cell concentration to fluorescence intensity, we mapped the profiles of protein-bound Trp fluorescence at 2,238, 2,954, 3,018, 3,036, and 3,000 m. Comparison of the fluorescence results and the cell counts (11) led to the following conversion factors: $C_{cells} = 1.52 \times 10^6\ cm^{-3} \times \langle I_{Trp} \rangle$, where $C_{cells}$ ($cm^{-3}$) is cell concentration and the brackets signify the fluorescence intensity averaged over ≈6 ml of ice. To relate the number of cells in an illuminated volume to fluorimeter intensity at that depth requires an estimate of the volume within which they are distributed. The volume within which a fluorimeter excites fluorescence is $\pi r_{beam}^2 \Delta z$. For the TUCS, with $r_{beam} \approx 100\ \mu m$ and $\Delta z \approx 0.5$ cm, $V_{TUCS} = 1.57 \times 10^{-4}$ $cm^3$. If the cells fill a volume $V \leq V_{TUCS}$, the number of cells in that volume element is $N_{cells} = 243 \times \langle I_{Trp} \rangle$. For typical intensities $\langle I_{Trp} \rangle = 0.02$ to 1.5 units, $C_{cells}$ ranges from $3.5 \times 10^4$ to $2.6 \times 10^6\ cm^{-3}$, and $N_{cells}$ ranges from ≈6 to 420 cells in $1.57 \times 10^{-4}$ $cm^3$. Background levels encountered in our scans of ice cores range from ≈0.002 to 0.005 unit, corresponding to 0.55 to 1.4 cells.

For more details, see *SI Materials and Methods*.

**ACKNOWLEDGMENTS.** We thank M. Bender, J. Severinghaus, R. Thauer, and J. Priscu for correspondence; and V. Miteva, T. Blunier, and B. Christner for reviews of the manuscript. This work was supported, in part, by National Science Foundation Grant ANT-0440609.

1. Priscu JC, Christner BC (2004) in *Microbial Diversity and Bioprospecting*, ed Bull AT (Am Soc Microbiol Press, Washington, DC), pp 130–145.
2. Price PB (2007) Microbial life in glacial ice and implications for a cold origin of life. *FEMS Microbiol Ecol* 59:217–231.
3. Sowers T (2001) $N_2O$ record spanning the penultimate deglaciation from the Vostok ice core. *J Geophys Res* 106:31903–31914.
4. Price PB, Sowers T (2004) Temperature dependence of metabolic rates for microbial growth, maintenance, and survival. *Proc Natl Acad Sci USA* 101:4631–4636.
5. Prospero JM, Blades E, Mathison G, Naidu R (2005) Interhemispheric transport of viable fungi and bacteria from Africa to the Caribbean with soil dust. *Aerobiologia* 12:1–19.
6. Flückiger J, *et al*. (1999) Variations in atmospheric $N_2O$ concentration during abrupt climatic changes. *Science* 285:227–230.
7. Flückiger J, *et al*. (2004) $N_2O$ and $CH_4$ variations during the last glacial epoch: Insight into global processes. *Global Biogeochem Cycles* 18:GB1020.
8. Spahni R, *et al*. (2005) Atmospheric methane and nitrous oxide of the late Pleistocene from Antarctic ice cores. *Science* 310:1317–1321.
9. Flückiger J (2003) Nitrous oxide and methane variations covering the last 100,000 years: insight into climatic and environmental processes. PhD thesis (University of Bern, Bern, Switzerland).
10. Campen RK, Sowers T, Alley RB (2003) Evidence of microbial consortia metabolizing within a low-latitude mountain glacier. *Geology* 31:231–234.
11. Tung HC, Bramall NE, Price PB (2005) Microbial origin of excess methane in glacial ice and implications for life on Mars. *Proc Natl Acad Sci USA* 102:18292–18296.
12. Tung HC, Price PB, Bramall NE, Vrdoljak G (2006) Microorganisms metabolizing on clay grains in 3-km-deep Greenland basal ice. *Astrobiology* 6:69–86.
13. Sowers T, Alley RB, Jubenville J (2003) Ice core records of atmospheric $N_2O$ covering the last 106,000 years. *Science* 301:945–948.
14. Chappellaz J, Brook E, Blunier T, Malaizé B (1997) $CH_4$ and $d^{18}O$ of $O_2$ records from Antarctic and Greenland ice: A clue for stratigraphic disturbance in the bottom part of the Greenland Ice Core Project and the Greenland Ice Sheet Project 2 ice cores. *J Geophys Res* 102:26547–26557.
15. Brook EJ, Sowers T, Orchardo J (1996) Rapid variations in atmospheric methane concentration during the past 110,000 years. *Science* 273:1087–1091.
16. DiMarco AA, Bobik TA, Wolfe RS (1990) Unusual coenzymes of methanogenesis. *Annu Rev Biochem* 59:355–394.
17. Purwantini E, Daniels L (1998) Molecular analysis of the gene encoding F420-dependent glucose-6-phosphate dehydogenase from *Mycobacterium smegmatis*. *J Bacteriol* 180:2212–2219.
18. Lin XL, White RH (1986) Occurrence of coenzyme $F_{420}$ and and its $\gamma$-monoglutamyl derivative in non-methanogenic archaebacteria. *J Bacteriol* 168:444–448.
19. Heine-Dobbernack E, Schoberth SM, Sahm H (1988) Relationship of intracellular coenzyme $F_{420}$ content to growth and metabolic activity of *Methanobacterium bryantii* and *Methanosarcina barkeri*. *Appl Environ Microbiol* 54:454–459.
20. Tison J-L, *et al*. (1998) Is a periglacial biota responsible for enhanced dielectric response in basal ice from the Greenland Ice Core Project ice core? *J Geophys Res* 103:18885–18894.
21. Souchez R, *et al*. (2006) Gas isotopes in ice reveal a vegetated central Greenland during ice sheet invasion. *Geophys Res Lett* 33:L24503.
22. Abysov SS, Mitskevich IN, Poglazova MN (1998) Microflora of the deep glacier horizon of central Antarctica. *Microbiology* 67:451–458.
23. Priscu JC, Downes MT, McKay CP (1996) Extreme supersaturation of nitrous oxide in a poorly ventilated Antarctic lake. *Limnol Oceanogr* 41:1544–1551.
24. Poughon L, Dussap C-G, Gros J-B (2001) Energy model and metabolic flux analysis for autotrophic nitrifiers. *Biotechnol Bioeng* 72:416–433.
25. Rohde RA, Price PB (2007) Diffusion-controlled metabolism for long-term survival of single isolated microorganisms trapped within ice crystals. *Proc Natl Acad Sci USA* 104:16592–16597.
26. Price PB (1995) Kinetics of conversion of air bubbles to air hydrate crystals in Antarctic ice. *Science* 267:1802–1804.
27. Raynaud D, Chappellaz J, Ritz C, Martinerie P (1997) Air content along the Greenland Ice Core Project core: A record of surface climatic parameters and elevation in central Greenland. *J Geophys Res* 102 (C12):26607–26613.
28. Suwa M, von Fischer JC, Bender ML, Landais A, Brook EJ (2006) Chronology reconstruction for the disturbed bottom section of the GISP2 and the GRIP ice cores: Implications for Termination II in Greenland. *J Geophys Res* 111:D02101.
29. Brinton KLF, Tsapin AI, Gilichinsky D, McDonald GD (2002) Aspartic acid racemization and age-depth relationships for organic carbon in Siberian permafrost. *Astrobiology* 2:77–82.
30. Lindahl T, Nyberg N (1972) Rate of depurination of native deoxyribonucleic acid. *Biochemistry* 11:3610–3618.
31. Mayewski PA, *et al*. (1997) Major features and forcing of high-latitude northern hemisphere atmospheric circulation using a 110,000-year-long glaciochemical series. *J Geophys Res* 102:26345–26366.
32. Steffensen JP (1997) The size distribution of microparticles from selected segments of the Greenland Ice Core Project ice core representing different climatic periods. *J Geophys Res* 102:26755–26763.
33. Petit JR, *et al*. (1999) Climate and atmospheric history of the past 420,000 years from the Vostok ice core, Antarctica. *Nature* 399:429–436.
34. Wolff EW, *et al*. (2006) Southern Ocean sea-ice extent, productivity and iron flux ove the past eight glacial cycles. *Nature* 440:491–495.
35. Bramall N (2007) The remote sensing of microorganisms. PhD thesis (University of California, Berkeley).
36. Maggi V (1997) Mineralogy of atmospheric microparticles deposited along the Greenland Ice Core Project ice core. *J Geophys Res* 102:26725–26734.
37. Clark CD, Zika RG (2000) in *Handbook of Environ Chem*, ed Wangersky P (Springer, Berlin), Vol 5, chap 1, pp 2–30.
38. Mopper K, Schultz CA (1993) Fluorescence as a possible tool for studying the nature and water column distribution of DOC components. *Mar Chem* 41:229–238.
39. Saltzman ES, Whung P-Y, Mayewski PA (1997) Methanesulfonate in the Greenland Ice Sheet Project 2 ice core. *J Geophys Res* 102:26649–26657.
40. Kurosaki Y, Mikami M (2007) Threshold wind speed for dust emission in east Asia and its seasonal variations. *J Geophys Res* 112:D17202.
41. Verbeke V, Lorrain R, Johnsen SJ, Tison J-L (2002) A multiple-step deformation history of basal ice from the Dye-3 (Greenland) core: New insights from the $CO_2$ and $CH_4$ content. *Ann Glac* 35:231–236.
42. Stauffer B, Flückiger J, Monnin E, Nakazawa T, Aoki S (2003) Discussion of the reliability of $CO_2$, $CH_4$ and $N_2O$ records from polar ice cores. *Mem Natl Inst Polar Res, Spec Issue* 57:139–152.
43. Johnson SS, *et al*. (2007) Ancient bacteria show evidence of DNA repair. *Proc Natl Acad Sci USA* 104:14401–14405.
44. Lindahl T (1993) Instability and decay of the primary structure of DNA. *Nature* 362:709–715.
45. Gazenko SV, Reponen TA, Grinshpun SA, Willeke K (1998) Analysis of airborne actinomycete spores with fluorogenic substrates. *Appl Environ Microbiol* 64:4410–4415.
46. Shafaat HS, Ponce A (2006) Applications of a rapid endospore viability assay for monitoring UV inactivation and characterizing Arctic ice cores. *Appl Environ Microbiol* 72:6808–6814.